

ESO Phase 3 Data Release Description

Data Collection	KIFF - 6 clusters
Release Number	1
Data Provider	Gabriel Brammer
Date	25.05.2016

Abstract

This release provides reduced K_s -band mosaics from the “KIFF” project: K_s -band Imaging of the *Hubble* Frontier Fields.

The first two fields, Abell 2744 and MACS-0416, were observed with HAWK-I on UT4 in P92 (092.A-0472) and the second two fields, Abell S1063, and Abell 370, were observed in P95 (095.A-0533). The quality of the final mosaics are quite uniform between all of the survey fields, reaching point source limiting magnitudes of $K_s \sim 26.0$ (AB, 5σ) and with superb image quality, FWHM $\sim 0.''4$ for point sources.

This data release also includes the two northern Frontier Fields clusters, MACS-0717 and MACS-1149, which were observed with shorter integrations with the *Keck*/MOSFIRE instrument in 2015 and 2016. The final mosaics of the 0717 and 1149 fields have image quality $\sim 0.''4$ and $0.''5$ and reach limiting depths $K_s = 25.5$ and 25.1 , respectively.

In all cases the K_s -band mosaics cover the primary cluster and parallel *HST*/ACS+WFC3 fields. The total area of the K_s -band coverage is 490 arcmin^2 . The K_s -band at $2.2 \mu\text{m}$ crucially fills the gap between the reddest *HST* filter ($1.6 \mu\text{m} \sim H$ band) and the *Spitzer*/IRAC $3.6 \mu\text{m}$ passband. While reaching the full depths of the space-based imaging is not currently feasible from the ground, the deep K_s -band images provide important constraints on both the redshifts and the stellar population properties of galaxies extending well below the characteristic stellar mass across most of the age of the universe, down to, and including, the redshifts of the targeted galaxy clusters ($z \sim 0.5$).

Overview of Observations

Table 1 summarizes the survey fields, instrument combinations, integration times and properties of the final mosaics. The HAWK-I observations offer a testament to the efficiency of service mode observations taken at the *VLT*: with total integration times of 25–29 hours for each field spread out over more than 30 OBs, the final mosaics all achieve nearly identical depths and superb image quality ($< 0.''4$ FWHM).

The $7' \times 7'$ field-of-view of the HAWK-I instrument is perfectly suited to simultaneously cover both the *HST* “cluster” and “parallel” areas with a single pointing. This requires two pointings with the *Keck*/MOSFIRE instrument. The layout of the K_s -band mosaics is shown in *Figure 1* below, compared to the footprints of the *Hubble* ACS and WFC3 instruments as well as *Spitzer* IRAC. For more information on the *Hubble* and *Spitzer* observations, see

<http://www.stsci.edu/hst/campaigns/frontier-fields/>

<http://ssc.spitzer.caltech.edu/warmmission/scheduling/approvedprograms/ddt/frontier/>

Field	z^a	R.A.	Dec.	Instrument	Epoch	<i>HST</i> ^b	t , hours	Depth ^c	FWHM
Abell 2744	0.31	00:14:21.2	-30:23:50	<i>VLT</i> /HAWK-I	2013 Oct 24–2013 Dec 24	C+P	29.3	26.0	0''39
MACS-0416	0.40	04:16:08.9	-24:04:28	<i>VLT</i> /HAWK-I	2013 Oct 25–2014 Feb 23	C+P	25.8	26.0	0''36
Abell S1063	0.35	22:49:01.1	-44:32:13	<i>VLT</i> /HAWK-I	2015 Jul 8–Sep 22	C+P	27.9	26.0	0''39
Abell 370	0.38	02:40:03.3	-01:36:23	<i>VLT</i> /HAWK-I	2015 Jul 26–2016 Jan 28	C+P	28.3	26.0	0''35
MACS-0717	0.55	07:17:34.0	+37:44:49	<i>Keck</i> /MOSFIRE	2015 Jan 26/27, 2016 Jan 21/22	C	4.3	25.3	0''42
						P	3.8	25.5	0''49
MACS-1149	0.54	11:49:36.3	+22:23:58	<i>Keck</i> /MOSFIRE	2015 Feb 24, 2016 Jan 21/22	C	5.5	25.2	0''53
						P	4.8	25.1	0''54
						<i>VLT</i> /HAWK-I ^d	2013 Mar 21–2014 Jun 9	C	5.3

Table 1: Summary of the KIFF *Ks*-band observations.

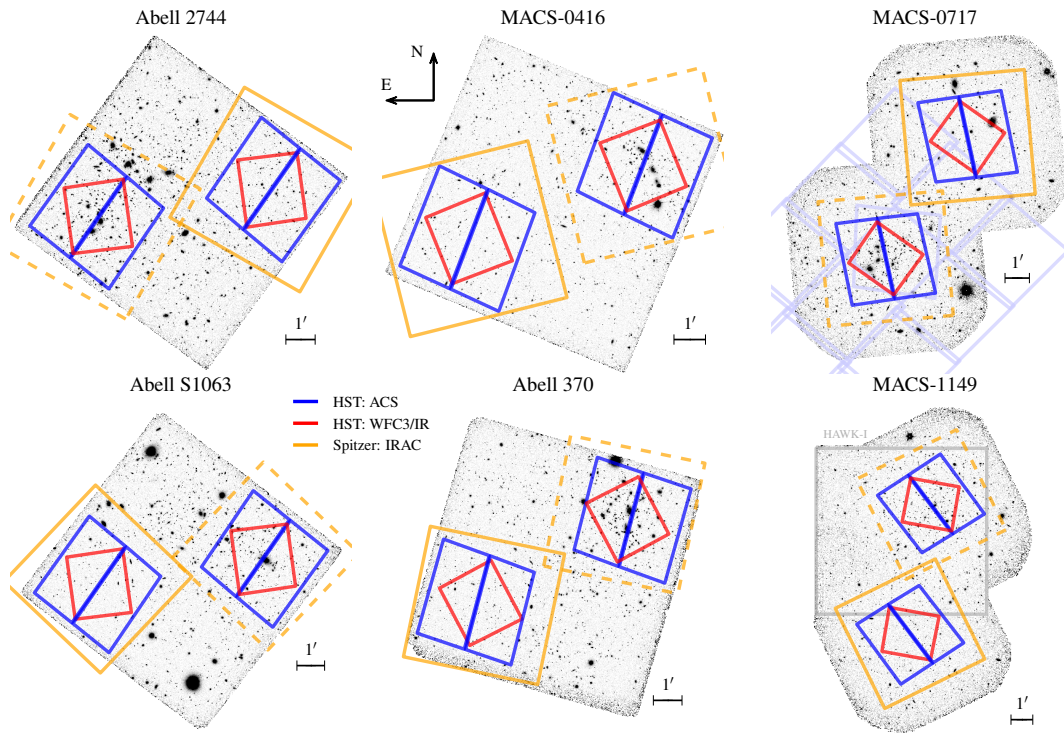


Figure 1: Layout of the KIFF survey fields, which cover the *Hubble* and *Spitzer* Frontier Fields cluster (yellow solid) and parallel (yellow dashed) pointings.

Release Content

This release comprises reduced *Ks*-band science and inverse-variance weight maps of the six survey fields. The total exposure times, observing data ranges, seeing and limiting magnitudes of the image mosaics are summarized in Table 1 above.

All of the images are drizzled (see the Data Reduction notes below) to a 0.1" pixel scale.

The images are photometrically calibrated with AB magnitude zeropoint 26.0.

Original Filename	R.A.	Decl.	Image Dimensions	File Size
KIFF_A2744_Ks_v1.0_sci.fits KIFF_A2744_Ks_v1.0_wht.fits	00:14:08.04	-30:23:21.8	11.6'×11.6' 7000×7000	187 Mb
KIFF_A370_Ks_v1.0_sci.fits KIFF_A370_Ks_v1.0_wht.fits	02:40:03.30	-01:36:23.3	10.5'×10.8' 6312×6500	157 Mb
KIFF_M0416_Ks_v1.0_sci.fits KIFF_M0416_Ks_v1.0_wht.fits	04:16:21.42	-24:05:40.6	10.8'×10.8' 6500×6500	161 Mb
KIFF_S1063_Ks_v1.0_sci.fits KIFF_S1063_Ks_v1.0_wht.fits	22:49:01.09	-44:32:12.7	12.3'×12.3' 7400×7400	209 Mb
KIFF_M0717_Ks_v1.0_sci.fits† KIFF_M0717_Ks_v1.0_wht.fits†	07:17:25.80	+37:47:05.8	12.6'×14.0' 7540×8400	242 Mb
KIFF_M1149_Ks_v1.0_sci.fits† KIFF_M1149_Ks_v1.0_wht.fits†	11:49:37.48	+22:20:37.8	11.7'×16.3' 7000×9800	262 Mb

† The MACS-0717 and MACS-1149 fields were observed primarily with *Keck*/MOSFIRE and therefore cannot have the same archive associations as the other fields obtained at the *VLT*. As they were obtained in a similar fashion and complete the *KIFF* coverage of all of the *HST* Frontier Fields, they are provided in this data release along with the other *VLT* fields. For archive processing they are indicated as associated attachments in the header of the “A370” science image and have the PRODCATG header values listed below. **To obtain the MOSFIRE fields you must request the A370 dataset from the archive query page, and they will be provided as attachments.** Check the README file provided with the archive retrieval request for a translation between the filenames listed in the tables here and the ESO archive filenames.

Filename	ASSON keyword in A370	PRODCATG	OBJECT
KIFF_M0717_Ks_v1.0_sci.fits	ASSON2	ANCILLARY.IMAGE	M0717
KIFF_M0717_Ks_v1.0_wht.fits	ASSON3	ANCILLARY.WEIGHTMAP	M0717
KIFF_M1149_Ks_v1.0_sci.fits	ASSON4	ANCILLARY.IMAGE	M1149
KIFF_M1149_Ks_v1.0_wht.fits	ASSON5	ANCILLARY.WEIGHTMAP	M1149

Release Notes

Data Reduction and Calibration

Flat-fielding and Sky Subtraction

The HAWK-I and MOSFIRE observations were reduced with a pipeline that has been developed for previous surveys with the NEWFIRM (NMBS; Whitaker et al. 2011) and FOURSTAR

(ZFOURGE; Straatman et al, submitted) infrared imaging instruments. Treating each detector individually, the pipeline is easily modified for the different instrument configurations of the four HAWK-I and single MOSFIRE chips. The primary task of the pipeline is removing the bright, time-variable sky background from the individual exposures, which is often more than 100 times brighter than the distant galaxies of interest in the field. With such a bright background, we first determine an empirical “sky flat” that is a median of all of the science exposures in a HAWK-I OB or MOSFIRE group, after rejecting the brightest 12 exposures at each pixel position to remove the contribution of bright objects. We find these empirical flats to be preferable to external twilight or dome flats given the difficulty of obtaining a truly flat illumination pattern over such large detector fields-of-view.

After dividing by the flat, the background of each exposure is determined in a first pass from the simple median of the four exposures that came both immediately before and after it. The background-subtracted exposures are combined into a mosaic from which objects are detected. The final refined background of each exposure is determined in a second “mask pass” from a median again from the four exposures before and after it but now aggressively masking all pixels that contain flux from the detected objects.

As the archival HAWK-I images of the MACS-1149 field were obtained with longer individual exposures and with fewer exposures per sequence, the mask-pass technique described above did not produce satisfactory results. In this case, for each raw exposure we divide by the empirical sky flat and then subtract a third-order polynomial fit to the background.

Photometric Calibration

For the HAWK-I observations, a single 90-minute Service Mode OB was obtained in each of the fields requiring photometric transparency conditions, and these OBs were followed immediately by an observation of a photometric standard star at a similar airmass with single exposures on each of the four chips. The standard star exposures were processed with the same pipeline used for the science exposures and the observed fluxes of the standard stars yield absolute photometric zeropoints for each chip. Correction factors were then computed to scale the OBs obtained at varying transparency levels to the calibrated photometric OB; the additional service mode OBs were obtained under generally satisfactory (i.e., “Clear”) weather conditions and the scale factors typically differ from unity by less than a few percent.

The 2-Micron All Sky Survey (2MASS) provides an additional check on the photometric calibration, though the comparison is limited due to relatively little brightness overlap between the faint end of reliable 2MASS photometry and the bright end where stars are in the linear regime of the detectors on the 8–10 m telescopes. We compared the magnitudes of point sources in the KIFF images to values in the 2MASS catalogs. We found good agreement in all fields and estimate a systematic uncertainty $\sigma_{\text{sys}} \leq 0.05$ mag for the photometric calibration.

We did not apply corrections for detector non-linearity and the image zeropoints (AB 26.0) **are not** corrected for Galactic extinction. The first correction is likely negligible for all of the galaxies in the field (though perhaps not for the brightest stars) and the Milky Way extinction is small in the near-infrared K_s band in these fields at relatively high Galactic latitude.

Astrometric Alignment

Reference absolute astrometric catalogs were generated from *HST* images when available (i.e., the chips overlapping the cluster and parallel *HST* fields, **Figure 1**) and public Subaru Suprime-Cam rc -band images otherwise. Transformations to the reference frame (shift, rotation and scale) were computed with the `stsci.stimage.xyymatch` and `scikit-image.transform` Python software tools for each background-subtracted exposure. For the HAWK-I exposures, we fit a third-order polynomial to the geometric distortion model determined by Libralato et al. (2014) and specify the polynomial terms as “Simple Imaging Polynomial” (SIP) coefficients (Shupe et al. 2005) in the individual exposure FITS files. The HAWK-I distortion is generally small, reaching

~ 2 pixels ($\sim 0.''2$) at the image corners, but the distortion corrections are necessary, in particular, given the excellent overall image quality of the observations.

Image Combination with “drizzle”

We combine all of the individual background-subtracted raw images (e.g., 7040 files for 1760 exposures in each of the four HAWK-I detectors for the Abell 2744 field) into the final output mosaic with the “drizzle” algorithm (Fruchter & Hook 2002, as implemented in the DrizzlePac + AstroDrizzle package; Gonzaga & et al. 2012). The drizzle implementation provides benefits over other methods in 1) trivial application of relative weights of the input images in creating the final mosaics, 2) providing infrastructure to apply the astrometric alignment and geometric distortion stored in the FITS headers, and 3) allowing the definition of an arbitrary output pixel grid without any additional image resampling.

We subtract a cell-based background from the final drizzled mosaics using an algorithm based on the background-subtraction used by SExtractor and SWarp but that provides more aggressive masking of flux in the outer isophotes of bright galaxies. We also compute the robust NMAD scatter (Brammer et al. 2008) of empty sky pixels within the same cells to empirically calibrate the inverse variance maps provided along with the science exposures.

With the drizzle implementation, the pixels of the individual raw exposures are resampled just one time, and even there the pixels are “shrunk” by a large factor before they are dropped into the output frame. This dramatically reduces correlated noise between neighboring pixels and the final result is that the inverse variance maps are well calibrated and can be used directly when computing uncertainties for photometry derived from the mosaics. For example, the expected variance of the sum of the pixel values within a given photometric aperture is simply the sum of the (inverse) inverse pixel variances.

Data Quality

Image Quality

We use point sources in the images to assess the image quality. *Figure 2* shows the curves of growth for stars identified in the field. Despite the compact cores of the stellar PSFs, the curves of growth shown in *Figure 2* deviate from Gaussian profiles with significantly higher flux in the outer wings, with a shape more consistent with a Moffat profile (Trujillo et al. 2001) with $\beta \sim 2$. We caution that these extended profiles will yield significantly shallower final image depths than would be predicted with the Exposure Time Calculator that may assume Gaussian profiles.

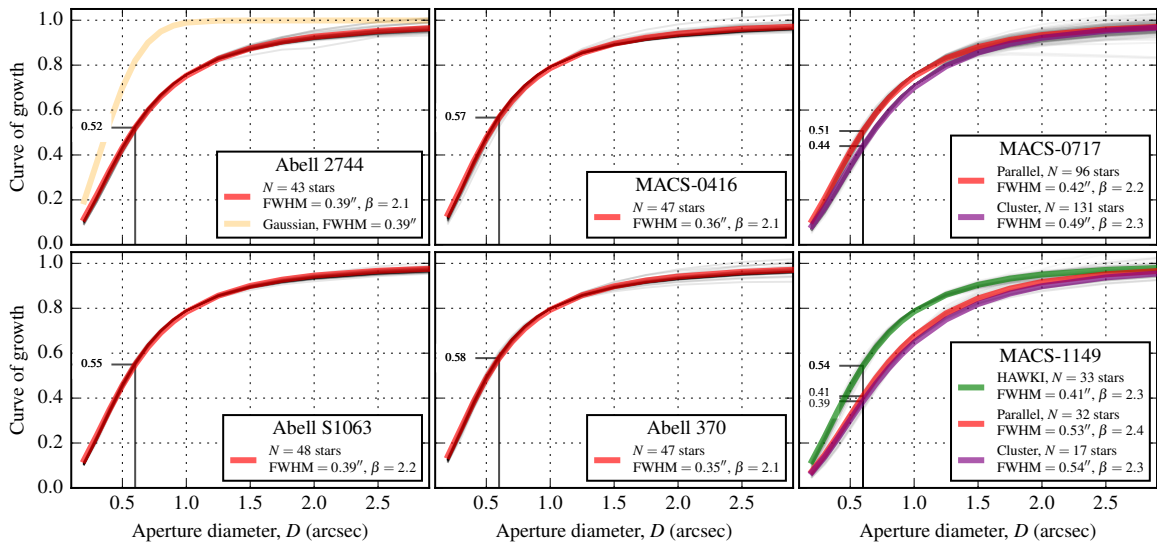


Figure 2: Curves of growth for point sources in the KIFF mosaics.

Depth

The product of the inverse of the curves of growth (i.e., aperture corrections) and the computed variance within a photometric aperture defines an optimal aperture size where this product is minimized (Whitaker et al. 2011). For our Ks-band mosaics, this optimal aperture has $D \sim 0.6''$, just larger than the FWHM of point-source profiles. The 5σ limiting magnitudes (AB) within $0.6''$ diameter apertures are indicated in *Figure 3* and listed in *Table 1*. Reaching 26th magnitude, the HAWK-I images presented here are among the deepest Ks-band images ever obtained (see also “HUGS”; Fontana et al. 2014) and they will provide an important complement to the deep HST and Spitzer imaging of the Frontier Fields.

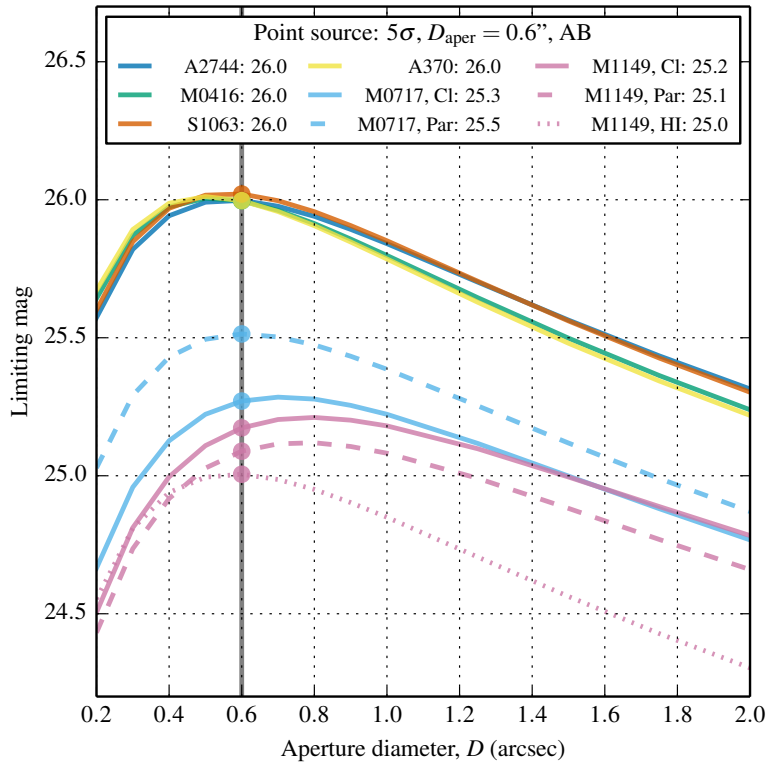


Figure 3: Limiting magnitude as a function of aperture diameter.

Data Format

File Types

The release files are all provided in standard FITS format.

Acknowledgements

The MOSFIRE images of the northern MACS-0717 and MACS-1149 were obtained through NASA Keck programs [N097](#) (2015) and N135 (2016), both PI: D. Marchesini, and with additional time contributed by M. Tanaka.

Full details of the observation log, data processing, and data quality have been submitted in a manuscript of the Astrophysical Journal Supplements:

“Ultra-Deep Imaging of the Hubble Frontier Fields”, 2016, ApJ-Submitted
Brammer, Marchesini, Labbé, Spitler, Lange-Vagle, Barker, Fontana, Galametz, Ferré-Mateu, Kodama, Lundgren, Martis, Muzzin, Stefanon, Tanaka, Toft, van der Wel, Vulcani, Whitaker

Please cite *Brammer et al., ApJSS-submitted* in any publications that make use of this KIFF data release, and please use the following statement in your articles when using these data, noting the programme IDs appropriate for the field(s) you wish to use:

Based on data products from observations made with ESO Telescopes at the La Silla Paranal Observatory under programme ID[s] 092.A-0472 [for *Abell 2744* and *MACS-0416*] and 095.A-0533 [for *Abell 370* and *Abell S1063*].